중전압 전동기 구동시스템을 위한 결합 인덕터를 갖는 플라잉 커패시터 MMC

리덕중, 이동춘
영남대학교 전기공학과

Flying-Capacitor Modular Multilevel Converters with Coupled Inductors for Medium-Voltage Motor Drive System

Duc Dung Le and Dong-Choon Lee
Dept. of Electrical Engineering, Yeungnam University

ABSTRACT

This paper proposes the coupled inductor instead of four non-coupled inductors in each leg of the flying-capacitor modular multilevel converter (MMC) to reduce the dimension, weight and cost of the magnetic core. The simulation results have verified the effectiveness of the proposed coupled inductor.

1. Introduction

MMC is regarded as one of the promising topologies for medium-voltage adjustable-speed AC motor drives. However, one issue for the MMC-fed motor drives is that the submodule (SM) capacitor voltage fluctuations are proportional to the output current and inversely proportional to the fundamental frequency [1], which limits the operating speed range of the motor.

In [1], the magnitude of capacitor voltage fluctuations at a low fundamental frequency was reduced by the injection of high-frequency common-mode voltage and circulating current. There are three types of injection of the high-frequency components such as the sinusoidal wave, the third-order harmonic, and the square wave. Those methods can fully eliminate the SM capacitor voltage fluctuations, but the common-mode voltage still remains as an issue in the motor side. It leads to the premature failure of winding insulation and motor bearing. A flying-capacitor MMC has been proposed in [2] to reduce the SM capacitor voltage ripples without injecting the common-mode voltage in the AC side. In [3], a flying-capacitor MMC with a center-tapped inductor coupling has been proposed to reduce the dimension, weight and cost of the magnetic core. However, the size and cost of the converter can be reduced by implementing the coupled inductor in each leg.

In this paper, a flying capacitor MMC with coupled inductors is proposed to reduce the dimension, weight and cost of the magnetic core. The validity of the proposed inverter is verified by simulation results for a 4160-V, 1250-hp IM drive system.

2. Flying-Capacitor MMC with Coupled Inductors

2.1 Circuit configuration and operating principle

Fig. 1(a) shows the circuit configuration of the flying-capacitor MMC with coupled inductors. Each arm is divided into two sub-arms with their conjunction node drawn out to connect with the flying capacitor C_F. The coupled inductor added in each leg is shown in Fig. 1(b), where $\phi_{a,u}$ and $\phi_{a,l}$ are the magnetic fluxes in the left-hand and right-hand side windings given as

$$\begin{bmatrix}\phi_{a,u}\\ \phi_{a,l}\end{bmatrix}=\begin{bmatrix}1 & -1 & \frac{1}{2} & -\frac{1}{2}\\ 1 & -1 & \frac{1}{2} & -\frac{1}{2}\end{bmatrix}\cdot\begin{bmatrix}\phi_1\\ \phi_2\\ \phi_3\\ \phi_4\end{bmatrix}. \quad (1)$$

The inductor voltages can be expressed as

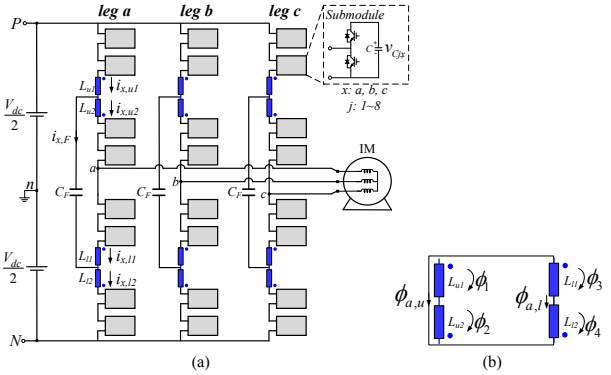

Fig. 1. Flying-capacitor MMC. (a) Circuit configuration. (b) Simplified representation of coupled inductor.

$$\begin{bmatrix}v_{Lu1}\\ v_{Ll1}\end{bmatrix}=-\begin{bmatrix}v_{Lu2}\\ v_{Ll2}\end{bmatrix}=L\frac{\partial}{\partial t}\begin{bmatrix}i_{x,u1}-i_{x,u2}+0.5i_{x,l1}-0.5i_{x,l2}\\ i_{x,l1}-i_{x,l2}+0.5i_{x,u1}-0.5i_{x,u2}\end{bmatrix}, \quad (2)$$

where v_{Lu1}, v_{Lu2}, v_{Ll1}, v_{Ll2}, $i_{x,u1}$, $i_{x,u2}$, $i_{x,l1}$ and $i_{x,l2}$ are the voltages and currents in each winding of the coupled inductor.

For the low speed operation, the high-frequency voltages generate high-frequency currents $i_{x,F}$ to redistribute the power difference between the upper and lower arms through the flying-capacitor C_F. Hence, the SM capacitor voltage ripples are kept within allowable ranges (lower than ±10% of v_C^*).

2.2 Control method

Fig. 2 shows the control block diagram of the flying-capacitor MMC, which consists of the motor speed control and the SM capacitor voltage control. Firstly, the motor-speed control is applied for a stable speed operation of the IM by generating the stator voltage references v_{as}^*, v_{bs}^* and v_{cs}^* based on the motor speed and currents, which is shown in Fig. 2(a). In order to achieve the desired magnitude and frequency of the stator voltages, the SM capacitor voltages have to be balanced by the SM capacitor voltage control. Secondly, the phase, arm and individual SM voltage balancing controls are employed to balance the SM capacitor voltages.

The control block diagram of the phase-voltage balancing control is shown in Fig. 2(b), where $\Delta v_{ph,x}^*$, v_C^* and $\bar{v}_{Cx}$ are the output voltage command, the SM capacitor voltage reference, and the average SM capacitor voltage of each phase, respectively. Additionally, the feedforward DC current $i_{d,fwd}$ and the DC current $i_{d,x}$ are given as

$$i_{d,fwd}=\frac{v_{s,x}\cdot i_x}{V_{dc}}, \quad (3)$$

$$i_{d,x}=0.5(i_{x,u2}+i_{x,l1}++i_{x,F}). \quad (4)$$

Fig. 2(c) shows the control block diagram of the arm-voltage

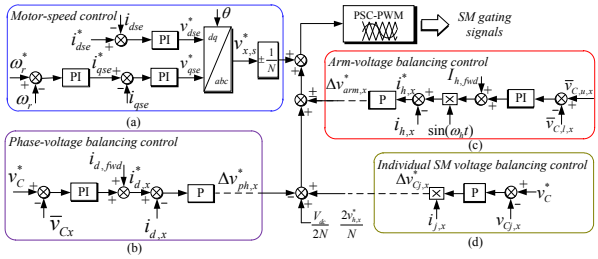

Fig. 2. Block diagrams for the SM capacitor voltage controls. (a) Motor speed control. (b) Phase-voltage balancing control. (c) Arm-voltage balancing control. (d) Individual SM voltage balancing control.

TABLE I CIRCUIT PARAMETERS FOR SIMULATION

Parameters	Symbol	Value
Converter		
DC-link voltage	V_{dc}	7000 V
Self-inductance	L	1.5 mH
Flying-capacitance	C_F	0.521 mF
Number of SMs per arm	N	4
SM capacitance	C	2000 μF
SM capacitor voltage reference	v_C^*	1750 V
Carrier frequency	f_c	2000 Hz
Injected frequency	f_h	180 Hz

balancing control, where $\bar{v}_{C,u,x}$ and $\bar{v}_{C,l,x}$ are the average SM capacitor voltages of the upper and lower arms, respectively. The high-frequency feedforward current $I_{h,fwd}$, and the high-frequency current $i_{h,x}$ are given, respectively, as

$$I_{h,fwd} = \frac{0.25V_{dc}\cdot i_x - v_{s,x}\cdot i_{d,fwd}}{V_h}, \quad (5)$$

$$i_{h,x} = \frac{i_{x,F}}{2}. \quad (6)$$

Fig. 2(d) shows the control block diagram of the SM individual voltage balancing control, where $v_{Cj,x}$ and $i_{j,x}$ are the capacitor voltage and current of each SM.

Finally, the phase-shift carrier modulation (PSC-PWM) is applied to generate the SM gating signals.

3. Simulation Results

In Table I, the converter parameters for the simulation are listed. Fig. 3 shows the simulation results with the load torque changes during the low-speed operation. Initially, the motor speed reference, n^*, is changed from standstill to 50 rpm (2.5 Hz) at no load. The amplitude of the start-up current (i_a, i_b, i_c) should be high enough to generate a start-up torque as shown in Fig. 3(a). During the speed acceleration, the SM capacitor voltages could become higher than the rated values ($v_{C,max} = 1.1v_C^*$ and $v_{C,min} = 0.9v_C^*$). In order to mitigate the SM capacitor fluctuations, the power difference between the upper and lower arms can be redistributed through the flying capacitor C_F. Fig. 3(b) shows the high-frequency current $i_{a,F}$ which flows through the flying capacitor C_F. Therefore, the SM capacitor voltage fluctuations are maintained within the allowable range as illustrated in Fig. 3(c), and the motor speed can follow its reference well as shown in Fig. 3(d).

At t = 0.75 s, the load torque is set to $T_L = 0.5T_{rated}$. Although the amplitude of the output current is increased, the SM capacitor voltages are still kept within the limitations. During this period, the power difference between the upper and lower arms becomes higher. Therefore, the amplitude of the high-frequency current, $i_{a,F}$, should be increased to mitigate the SM capacitor voltage ripples. When a full load is applied at t = 1.25 s, the SM capacitor voltage ripples are alleviated and the motor speed still tracks the reference well.

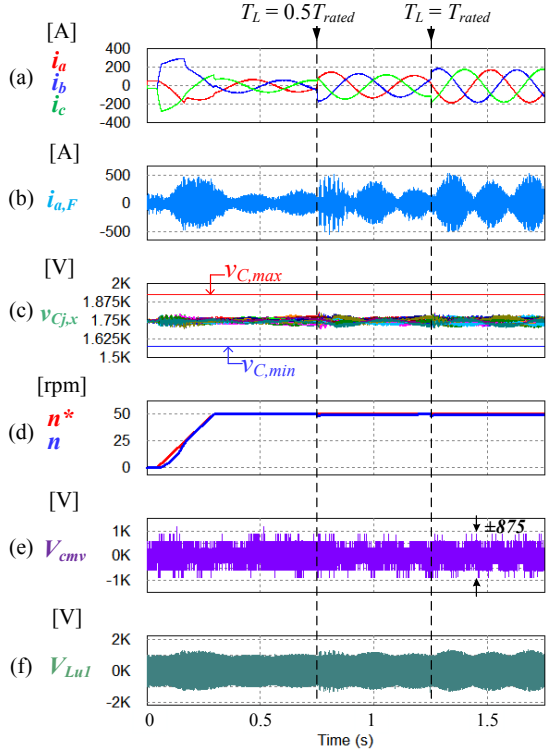

Fig. 3. System performance at low-speed operation. (a) Three-phase current. (b) High-frequency current. (c) SM capacitor voltages. (d) Motor speed. (e) Common-mode voltage. (f) Winding voltage V_{Lu1}.

Fig. 3(e) shows the common-mode voltage, $v_{cmv} = (v_{an} + v_{bn} + v_{cn})/3$, at the motor side, which has a value of ±875 V ($\pm 0.5v_C^*$). This value is similar to that of the topology without coupled inductors [2]. In Fig. 3(f), the winding voltage, V_{Lu1}, in the right-hand side of the coupled is shown with a peak value of ±1250 V.

4. Conclusions

This paper has proposed a flying-capacitor MMC with the coupled inductors for the induction motor drives systems, where the dimension, weight and cost of the magnetic core can be reduced, compared with the non-coupled inductors. The simulation results have confirmed the feasibility of the proposed coupled inductor. A stable operation of induction motor drives at a low-speed region has been obtained with the allowable SM capacitor voltage ripples.

This work was supported by the Korea Institute of Energy Technology Evaluation and Planning (KETEP) and the Ministry of Trade, Industry & Energy (MOTIE) of the Republic of Korea (No.217C000289).

References

[1] A. J. Korn, M. Winkelnkemper, and P. Steimer, "Low output frequency operation of the modular multi-level converter," *Proc. IEEE ECCE.*, pp. 3993–3997, 2010.

[2] S. Du, B. Wu, N. R. Zargari, and Z. Cheng, "A flying-capacitor modular multilevel converter for medium-voltage motor drive," *IEEE Trans. Power Electron.*, vol. 32, no. 3, pp. 2081–2089, 2017.

[3] D. D. Le and D. C. Lee, "Flying-capacitor modular multilevel converters with coupled inductors," *in proc. of KIPE Conf.*, pp. 288–289, 2018.